

# Ab initio molecular dynamics investigation of the structure and the noncollinear magnetism in liquid oxygen: Occurrence of O<sub>4</sub> molecular units

著者	Oda Tatsuki, Pasquarello Alfredo
journal or publication title	Physical Review Letters
volume	89
number	19
page range	197204
year	2002-11-04
URL	<a href="http://hdl.handle.net/2297/14406">http://hdl.handle.net/2297/14406</a>

doi: 10.1103/PhysRevLett.89.197204

## ***Ab Initio* Molecular Dynamics Investigation of the Structure and the Noncollinear Magnetism in Liquid Oxygen: Occurrence of O<sub>4</sub> Molecular Units**

Tatsuki Oda<sup>1</sup> and Alfredo Pasquarello<sup>2,3</sup>

<sup>1</sup>*Department of Computational Science, Faculty of Science, Kanazawa University, Kanazawa 920-1192, Japan*

<sup>2</sup>*Institut de Théorie des Phénomènes Physiques (ITP), Ecole Polytechnique Fédérale de Lausanne (EPFL), CH-1015 Lausanne, Switzerland*

<sup>3</sup>*Institut Romand de Recherche Numérique en Physique des Matériaux (IRRMA), CH -1015 Lausanne, Switzerland*  
(Received 17 April 2002; published 21 October 2002)

We modeled liquid oxygen using *ab initio* molecular dynamics in which both the atomic structure and the noncollinear magnetic structure evolve without constraints. The atomic structure shows preference for parallel alignment of first-neighbor molecules and is supported by an excellent agreement between theoretical and experimental nuclear structure factors. The magnetic structure shows short-range antiferromagnetic correlations in agreement with spin-polarized neutron diffraction data. The observed correlations primarily result from appropriate trajectories of colliding O<sub>2</sub> molecules. The simulation provides evidence for the occurrence of long-living O<sub>4</sub> molecular units.

DOI: 10.1103/PhysRevLett.89.197204

PACS numbers: 71.15.Pd, 61.20.Ja, 61.25.Em, 75.50.Mm

While noncollinear spin arrangements have been observed in a variety of materials [1,2], their occurrence has remained poorly understood. Noncollinear magnetism is expected to be strongly affected by the underlying atomic structure, occurring more easily for systems of low symmetry or in a disordered state. In this respect, the liquid state offers the possibility of investigating the magnetism for a continuously evolving atomic structure. The development of appropriate theoretical tools for addressing the noncollinear magnetism in such systems constitutes a theme of great current interest [1,2].

A magnetic fluid of particular interest is liquid oxygen, in which the individual molecular units preserve the magnetic state they carry in the gas phase. On the basis of magnetic susceptibility data [3], Lewis postulated the dimerization of some oxygen molecules in the liquid [4], leading to the formation of O<sub>4</sub> molecules in a magnetically saturated state. The chemical bonding in the O<sub>4</sub> molecule is quite particular [5], since the unpaired electrons of the O<sub>2</sub> molecules remain in an open-shell structure upon bonding. Neutron diffraction experiments on liquid oxygen are sensitive to both the atomic and the magnetic structure [6–8] but are unable to reveal the occurrence of long-living O<sub>4</sub> units. Using spin-polarized neutrons, Deraman *et al.* separated the two components and found antiferromagnetic ordering at short-range distances [9], which might be taken as indirect evidence for O<sub>4</sub> formation. However, since the temperature exceeds estimates of the magnetic interactions by more than one order of magnitude, the observed antiferromagnetism appeared surprising [9].

To investigate the noncollinear magnetic structure [10] and its correlation with evolving atomic positions, we here combined *ab initio* molecular dynamics [11] and an energy functional in which the magnitude and the direction of the magnetization are continuous functions of spatial position [2]. This energy functional was previously

successfully used to determine the noncollinear magnetic structures of small iron clusters by combined electronic and structural relaxation [2]. Applied to liquid oxygen, this scheme allows us to follow simultaneously the evolution of the atomic, electronic, and magnetic structure within a unique and consistent theoretical framework.

We modeled liquid oxygen by a system composed of 32 molecules in a periodically repeated cubic cell of side 11.4 Å, at the experimental density of 1.14 g/cm<sup>3</sup> [12]. The electronic structure was described within a generalized gradient approximation (PW91) for the exchange-correlation energy [13]. We used an ultrasoft pseudopotential scheme [14,15] in which the O 1s state was included in the core. The valence wave functions and the augmented electron density were expanded on plane-wave basis sets defined by energy cutoffs of 25 and 150 Ry, respectively. The Brillouin-zone sampling was restricted to the  $\Gamma$  point, as justified by the molecular nature of the liquid [16]. With these parameters, we obtained for the isolated molecule in its triplet state a bond length of 1.25 Å, a vibrational frequency of 43.6 THz, and a binding energy of 5.84 eV, in satisfactory agreement with experimental values (1.21 Å, 47.4 THz, and 5.12 eV) [17].

The simulation was started from an initial atomic configuration, in which the atomic vibrations in the molecules were given a random phase. Then, after a brief annealing cycle to high temperatures, the temperature was fixed at 90 K by switching on thermostats on both nuclear and electronic degrees of freedom [18]. The fictitious mass [11] was set to 200 a.u. and the motion was integrated with a time step of 0.24 fs. Overall, the simulation spanned a time period of 19 ps, but only the last 14 ps were used for averages of physical properties. For this system, the computational cost for treating the noncollinear magnetic structure is higher by a factor of  $\sim 13$  with respect to the non-spin-polarized case [19].

To ensure rapid thermalization, the evolution of the atomic positions was coupled to three different Nosé thermostats [20] which controlled separately the temperature of translational, rotational, and vibrational motions. This setup ensured thermal fluctuations in the range of a few tens of degrees. To keep electronic excitations under control, we also used a thermostat coupled to the electronic variables, which fixed the average fictitious kinetic energy to 79 meV. On six occasions during the course of the simulation, without interrupting its continuous evolution, we determined the excitation energy with respect to the Born-Oppenheimer energy surface [11]. We found an average excitation energy of 4.2 meV, with the largest excitation energy of 10 meV. These values are well below both the average thermal energy and typical fluctuations of the total interaction energy, thereby ensuring a correct description of the evolution.

The evolution of the average mean square displacement was typical of diffusive motion in a liquid and gave an estimate for the diffusion constant of  $2.3 \pm 0.2 \times 10^{-5}$  cm<sup>2</sup>/s [21]. The nuclear structure factor was obtained as average over structural configurations in the simulation (Fig. 1). The calculated structure factor closely reproduces all the significant features observed in the experimental one [7,22]. These include the main peak at about  $2 \text{ \AA}^{-1}$ , the shoulder at  $4 \text{ \AA}^{-1}$ , and the broad peak around  $6 \text{ \AA}^{-1}$ . The main peak is caused by coherent intermolecular diffraction, while the oscillation extending beyond transferred momenta of  $\sim 5 \text{ \AA}^{-1}$  mainly results from intramolecular diffraction. We found that the shoulder at  $4 \text{ \AA}^{-1}$  could not be reproduced within a model of the liquid assuming uncorrelated molecular orientations [7]. In fact, this shoulder results from incoherent intermolecular scattering, and its appearance is a signature of a preferential relative orientation of nearest-neighbor molecules (mainly *H*- and *X*-type, *vide infra*).

Figure 2 shows the radial distribution function  $g(r)$  of nuclear positions, together with that of the centers of O<sub>2</sub> molecules. The sharp peak at  $1.24 \text{ \AA}$  corresponds to the

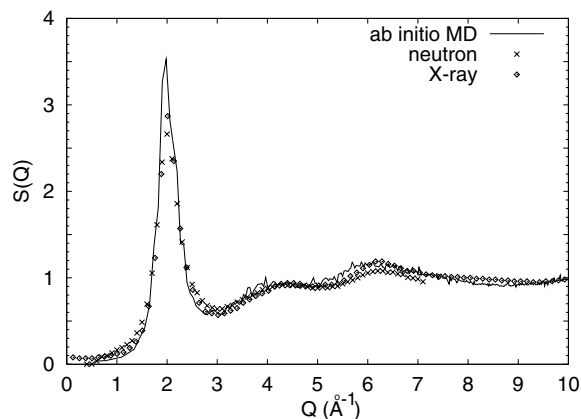


FIG. 1. Nuclear structure factor (solid line). The data points are from neutron [7] (crosses) and x-ray diffraction measurements [22] (diamonds).

distance between oxygen atoms within the same O<sub>2</sub> molecule. The distribution of atoms belonging to different molecular units shows peaks at 3.6 and 6.8 Å, separated by a minimum at 5.3 Å. The shoulder at about 4.1 Å corresponds to second nearest atoms in first-neighbor molecules. All these features were also found in the experimentally derived correlation function [8], which is overall well reproduced by our results (not shown). The first shell of molecules defined by the first minimum contains 13.0 molecules.

To describe the relative orientation of O<sub>2</sub> molecules in the liquid, we introduced the following order parameters:  $p_a = \sin^2\theta_1 \sin^2\theta_2 \cos^2\varphi$  (*H*-type),  $p_b = \sin^2\theta_1 \sin^2\theta_2 \times \sin^2\varphi$  (*X*-type),  $p_c = (\sin^2\theta_1 \cos^2\theta_2 + \cos^2\theta_1 \sin^2\theta_2)$  (*T*-type), and  $p_d = \cos^2\theta_1 \cos^2\theta_2$  (*I*-type), where  $\theta_1$  and  $\theta_2$  are polar angles with respect to the axis connecting the centers of a pair of molecules, and  $\varphi$  is the dihedral angle between the planes containing the molecular axes and the connecting axis. We calculated averaged order parameters as a function of distance  $r$  between two O<sub>2</sub> molecules:

$$\langle p_\alpha \rangle = \left\langle \frac{\sum_{ij} p_\alpha(\theta_1, \theta_2, \varphi) \delta(r - r_{ij})}{\sum_{ij} \delta(r - r_{ij})} \right\rangle, \quad (1)$$

where  $\alpha$  specifies one of the order parameters, and  $r_{ij}$  is the distance between the  $i$ th and  $j$ th molecules. Figure 3 shows that the *H*-type (rectangular) geometry stands out as the preferred one at short-range distances, as is also the case in the gaseous phase [23]. For distances beyond 4 Å, all the averaged order parameters do not differ significantly from their respective values for uncorrelated orientations.

The simulation shows local moments rotating without pointing into any preferential direction. This is consistent with paramagnetic behavior, which results in a vanishing average magnetization in the absence of an external

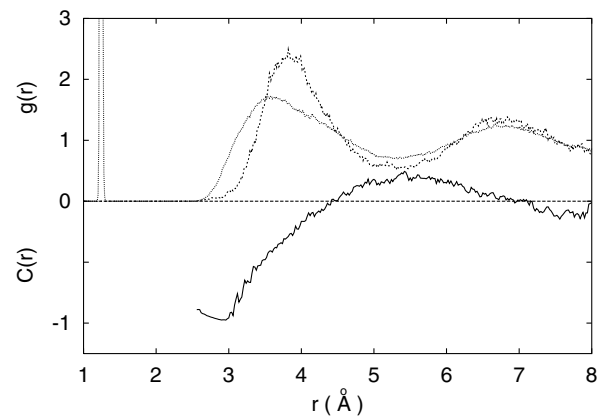


FIG. 2. Upper panel: radial distribution functions for atomic positions (dotted line) and for the centers of O<sub>2</sub> molecules (dashed line). Lower panel: magnetic correlation function (solid line) for molecular magnetic moments.

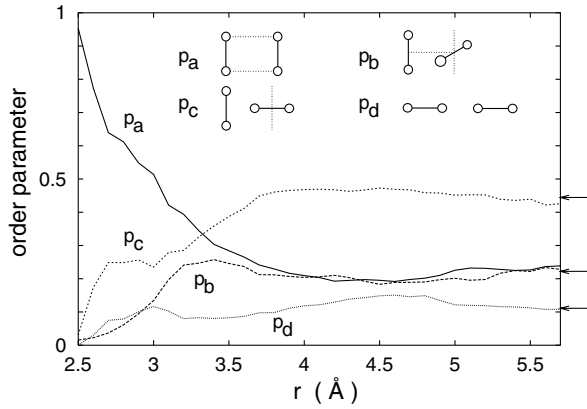


FIG. 3. Averaged order parameters (see text) as a function of distance between  $O_2$  molecules. The arrows specify the values for uncorrelated orientations.

magnetic field. The average total magnetization  $\langle \mathbf{M}_{\text{tot}} \rangle$  in the simulation was found to be  $(-0.03, -0.03, 0.34)\mu_B$  per cell. Other averages gave  $\langle |\mathbf{M}_{\text{tot}}| \rangle = 3.1\mu_B$  and  $\langle |\mathbf{M}_{\text{tot}}|^2 \rangle = 11.7\mu_B^2$ . These values are negligible with respect to the values associated to the hypothetical ferromagnetic alignment.

Before addressing the magnetic structure factor, it is instructive to consider the magnetic correlation function in real space  $C(r)$ ,

$$C(r) = \left\langle \frac{\sum_{i \neq j} \mathbf{m}_i \cdot \mathbf{m}_j \delta(r_{ij} - r)}{\sum_{ij} \mu^2 \delta(r_{ij} - r)} \right\rangle, \quad (2)$$

where  $\mathbf{m}_i$  is the magnetic moment of the  $i$ th molecule and  $\mu$  its average. Molecular magnetic moments were found to be meaningful when integrating the spin density  $\mathbf{m}(\mathbf{r})$  within two spheres of radius  $0.69 \text{ \AA}$  centered on the respective atoms. The function  $C(r)$  shows well defined magnetic correlations (Fig. 2, lower panel). At distances corresponding to nearest-neighbor molecules, antiferromagnetic correlations dominate and appear to saturate for distances lower than  $3.1 \text{ \AA}$ . At larger distances, in correspondence of the first minimum of the radial distribution function (between  $4.4$  and  $7.0 \text{ \AA}$ ), the correlations turn ferromagnetic.

The differential cross section of spin-polarized neutrons diffracted by the electron spin density is given by  $d\sigma/d\Omega = sI(Q)$ , where  $s$  is the squared scattering length per molecule and  $I(Q)$  the magnetic structure factor:

$$I(Q) = \frac{2}{N\mu_0^2} \left\langle \left| \int d\mathbf{r} \mathbf{m}(\mathbf{r}) \exp(-i\mathbf{Q} \cdot \mathbf{r}) \right|^2 \right\rangle, \quad (3)$$

in which  $\mu_0$  is the magnetic moment of an isolated molecule. To gain insight, it is useful to express  $I(Q)$  in terms of molecular form factors. Assuming that the orientation of a pair of molecules is decoupled from the direction of their connecting axis, we obtain

$$I^{\text{approx}}(Q) = F_{m1}(Q) + F_{m2}(Q)[S_m(Q) - 1], \quad (4)$$

where  $F_{m1}(Q) = \langle |\mu(Q)|^2 \rangle / \mu_0^2$  and  $F_{m2}(Q) = \langle |\mu(Q)\rangle|^2 / \mu_0^2$  are molecular magnetic form factors known as Kleiner's factors [24], and  $S_m(Q) = 2\langle |\sum_i \mathbf{m}_i e^{-i\mathbf{Q} \cdot \mathbf{r}_i}|^2 \rangle / N\mu_0^2$  is related by Fourier transformation to the real-space correlation  $C(r)$  in Eq. (2) [9]. From the simulation, we obtained both  $I(Q)$  and  $I^{\text{approx}}(Q)$  and found that the two quantities are hardly distinguishable. The magnetic structure factor  $I(Q)$  can therefore reliably be interpreted in terms of molecular form factors and of  $S_m(Q)$ , which depends solely on the directions of the local molecular magnetizations.

The structure factor  $I(Q)$  averaged over configurations in the simulation and the corresponding one measured by neutron diffraction [9] are compared in Fig. 4. It is convenient to interpret  $I(Q)$  in terms of deviations with respect to  $F_{m1}(Q)$  to which it converges for large  $Q$ . Both the theoretical and the experimental  $I(Q)$  show a well defined dip around  $2 \text{ \AA}^{-1}$ , while only a shoulder occurs in the experimental  $I(Q)$  in correspondence of the large peak at  $1.2 \text{ \AA}^{-1}$  in the calculated  $I(Q)$ . The modulation of  $I(Q)$  with respect to  $F_{m1}(Q)$  results from the structure in  $S_m(Q)$  (Fig. 4, inset). By separating the contribution to  $S_m(Q)$  from molecules at different distances, we found that the dip around  $2 \text{ \AA}^{-1}$  originates from the short-range antiferromagnetic correlations, whereas the peak at  $1.2 \text{ \AA}^{-1}$  contains contributions from both antiferromagnetic and ferromagnetic correlations. These results indicate that we can infer the occurrence of short-range antiferromagnetic correlations directly from the experimental data points, without relying on a real-space transform based on a limited range of  $Q$  values [9].

The differences between the theoretical and experimental  $I(Q)$  for  $Q < 1.4 \text{ \AA}^{-1}$  result from the neglect of thermal electronic excitations in the simulation, as a consequence of the use of the Born-Oppenheimer

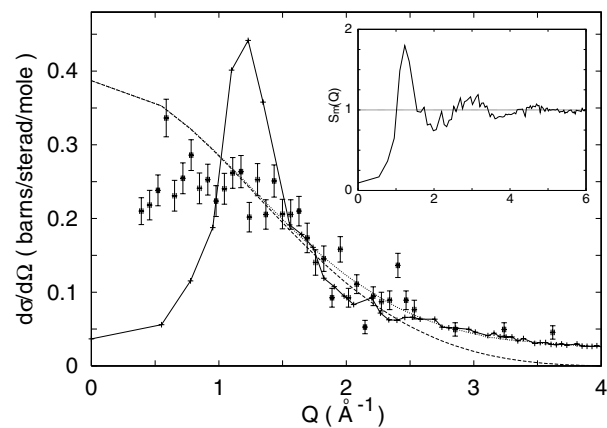


FIG. 4. Differential cross section (solid line) of elastic neutron scattering calculated from the full spin density in liquid oxygen, and the experimental result of Deraman *et al.* [9] (data with error bars). The molecular form factors,  $sF_{m1}(Q)$  (dotted line) and  $sF_{m2}(Q)$  (dashed line). For all cases, the factor  $s = 0.387 \text{ b/sr}$  is used as cross section per molecule. Inset: magnetic structure factor  $S_m(Q)$  associated to molecular centers.

approximation [11]. In fact, as  $Q$  goes to zero,  $I(Q)$  can be related to the isothermal magnetic susceptibility  $\chi(T)$  [25], which results primarily from electronic excitations. From experimental susceptibility data [3], we estimate a value of  $0.24 \pm 0.03$  for  $sI(0)$  [25], in good agreement with the polarized neutron diffraction data of Deraman *et al.* [9]. The effect on  $I(Q)$  associated to electronic excitations is likely to extend to finite  $Q$  values. Assuming a Heisenberg model for spin coupling, it is straightforward to deduce that thermal magnetic fluctuations tend to oppose the zero-temperature spin alignment. Hence, these effects would generally result in an experimental  $I(Q)$  with a reduced structure with respect to the  $I(Q)$  obtained from the simulation, offering a plausible explanation for the observed differences.

At short-range distances, both the static *structural* and *magnetic* properties are consistent with the formation of  $O_4$  molecular units in the liquid. We now address the stability of such units. Using a procedure similar to the one proposed in Ref. [26], we found an averaged residence time  $\tau$  of 0.16 ps for two molecules remaining within a radius  $r_c = 3.1 \text{ \AA}$ . To check the dependence of the residence time on the relative orientation of two molecules, we selected pairs of molecules on the basis of the order parameters defined above. Focusing on  $H$ -type geometries, we found  $\tau_H = 0.20$  ps, which does not differ significantly from the residence time associated to pairs colliding with other orientations ( $\tau_{\text{other}} = 0.11$  ps). This analysis fully supports the conjecture of Deraman *et al.* that the short-range antiferromagnetic correlations result from collisions with appropriate trajectories [9]. Moreover, the simulation reveals the occurrence of four  $O_4$  units which survive for more than 0.6 ps. The residence time of the longest living  $O_4$  unit ( $\tau = 0.8$  ps) is found to be comparable with the experimental lifetime in the gaseous phase (1 ps) [27].

In conclusion, we performed *ab initio* molecular dynamics to investigate the noncollinear magnetism of a system with an evolving atomic structure. Application to liquid oxygen provides us with a picture in which the large majority of colliding  $O_2$  molecules assume structural and magnetic configurations which closely resemble those in the  $O_4$  molecule. Formation of truly long-living molecular  $O_4$  units also occurs but involves a considerably smaller fraction of  $O_2$  molecules.

Support is acknowledged from the Japanese Society for the Promotion of Science under Project No. 11694066 (T.O.), the Swiss National Science Foundation under Grant No. 620-57850.99 (A.P.), and the Swiss Center for Scientific Computing (CSCS).

- [1] L. Nordström and D. J. Singh, Phys. Rev. Lett. **76**, 4420 (1996); V. P. Antropov, B. N. Harmon, and A. N. Smirnov, J. Magn. Magn. Mater. **200**, 148 (1999); D. M. Bylander and L. Kleinman, Phys. Rev. B **59**, 6278 (1999);

- K. Knöpfle, L. M. Sandratskii, and J. Kübler, Phys. Rev. B **62**, 5564 (2000); R. Gebauer *et al.*, Phys. Rev. B **61**, 6145 (2000); H. Yamagami, Phys. Rev. B **61**, 6246 (2000); D. Hobbs, G. Kresse, and J. Hafner, Phys. Rev. B **62**, 11 556 (2000).
- [2] T. Oda, A. Pasquarello, and R. Car, Phys. Rev. Lett. **80**, 3622 (1998).
- [3] A. Perrier and H. Kamerlingh Onnes, Phys. Comm. Leiden **139c-d**, 25 (1914).
- [4] G. N. Lewis, J. Am. Chem. Soc. **46**, 2027 (1924).
- [5] L. Pauling, *The Nature of the Chemical Bond and the Structure of Molecules and Crystals: An Introduction to Modern Structural Chemistry* (Cornell University, New York, 1960), p. 353.
- [6] D. G. Henshaw, Phys. Rev. **119**, 22 (1960).
- [7] J. C. Dore, G. Walford, and D. I. Page, Mol. Phys. **29**, 565 (1975); P. A. Egelstaff, D. I. Page, and J. G. Powles, Mol. Phys. **20**, 881 (1971).
- [8] J. H. Clarke, J. C. Dore, and R. N. Sinclair, Mol. Phys. **29**, 581 (1975).
- [9] M. Deraman, J. C. Dore, and J. Schweizer, J. Magn. Magn. Mater. **50**, 178 (1985).
- [10] U. von Barth and L. Hedin, J. Phys. C **5**, 1629 (1972).
- [11] R. Car and M. Parrinello, Phys. Rev. Lett. **55**, 2471 (1985).
- [12] *CRC Handbook of Chemistry and Physics*, edited by Robert C. Weast (CRC Press, Cleveland, 1977), p. F-80.
- [13] J. P. Perdew *et al.* Phys. Rev. B **46**, 6671 (1992).
- [14] D. Vanderbilt, Phys. Rev. B **41**, 7892 (1990).
- [15] A. Pasquarello *et al.*, Phys. Rev. Lett. **69**, 1982 (1992); K. Laasonen *et al.*, Phys. Rev. B **47**, 10142 (1993).
- [16] By considering several configurations of the liquid, we calculated an average energy gap of 1.9 eV, only slightly lower than for the isolated  $O_2$  (2.4 eV).
- [17] K. P. Huber and G. Herzberg, *Molecular Spectra and Molecular Structure: IV. Constants of Diatomic Molecules* (Van Nostrand Reinhold, New York, 1979), p. 490.
- [18] P. E. Blöchl and M. Parrinello, Phys. Rev. B **45**, 9413 (1992).
- [19] This increase results mostly from matrix multiplications involving the wave functions, which are no longer real.
- [20] S. Nosé, Mol. Phys. **52**, 255 (1984); W. G. Hoover, Phys. Rev. A **31**, 1695 (1985).
- [21] Despite its dynamical nature, the diffusion coefficient is generally not severely affected by thermostats [20].
- [22] H. W. Furumoto and C. H. Shaw, quoted in *Simple Dense Fluids*, edited by H. L. Frisch and Z. W. Salsburg (Academic, New York, 1968), p. 80.
- [23] L. Biennier *et al.*, J. Chem. Phys. **112**, 6309 (2000); V. Aquilanti *et al.*, Phys. Rev. Lett. **82**, 69 (1999).
- [24] W. H. Kleiner, Phys. Rev. **97**, 411 (1960).
- [25] To estimate  $I(0) = 3k_B T \chi(T) / 8\mu_B^2$ , where  $k_B$  and  $T$  are the Boltzmann constant and the temperature, respectively, we used measured data of  $\chi(T)$  [3] for  $T$  between 54 and 90 K.
- [26] R. W. Impey, P. A. Madden, and I. R. McDonald, J. Phys. Chem. **87**, 5071 (1983).
- [27] C. A. Long and G. E. Ewing, Chem. Phys. Lett. **9**, 225 (1971).